Preprints (www.preprints.org) | NOT PEER-REVIEWED | Posted: 30 September 2020

## I. INTRODUCTION

As a strange celestial body, the study of black holes has always attracted the attention of physicists. Last year, through a project called Event Horizon Telescope (EHT), mankind got the first image of the shadow of the M87 supermassive black hole (SMBH) [1–6], which led us into a new era of black hole physics. It is foreseeable that with the improvement of the level of observation and the acquisition of more experimental data, we will have a deeper understanding of the nature of black holes, which will also provide scientists with feasible methods to test different gravitational theories.

In order to study the nature of black holes, we must determine the photon regions firstly. In Schwarzschild case, the black hole remains stationary, photons with critical angular momentum will form a stable spherical photon sphere near the black hole at this time [7, 8], which is an area filled with null geodesics. But in Kerr case, the black hole starts to rotate, and the null geodesics no longer remain spherical. The spherical photon sphere is split into photon regions [9, 10], and these approximately circular null geodesics describe the boundary of the black hole shadow. So the nature of photon regions take great significance to the research of black hole shadow.

The black hole shadow is one of the important conclusions of the general gravitational theory. It is formed by the null geodesics in the strong gravitational region near the black hole. A photon with a large angular momentum flying from infinity, due to the influence of the strong gravitational force of the black hole, the path of motion will be deflected and eventually fly to infinity. There is evidence that a massive black hole exists in the center of the galaxy. Since the galaxies are rotating, it is very likely that the black hole is also rotating. Spin and mass are two important parameters for studying the properties of black holes, and black hole shadow is one of the effective methods to observe the spin and mass of black holes. The existence

Preprints (www.preprints.org) | NOT PEER-REVIEWED | Posted: 30 September 2020

of black hole shadow was first studied by bardeen [11]. The black hole shadow in Schwarzschild case [12–15], the rotating black hole with electric charge [9] or gravitomagnetic and other spherically symmetric black holes have been extensively studied. It has been demonstrated that the black hole shadow in Schwarzschild case is a perfect circle [16] in vacuum [17] or in plasma [18, 19]. But in rotating case, since the black hole has angular momentum, the shadow will be deformed [20–27]. Shadows of Kerr-Newman black holes were obtained in [27], while the naked singularities with deformation parameters was discussed in [28], multi-black holes [29] and Kerr-Taub-NUT black hole in [30]. These works are also used to study other black hole or wormhole backgrounds [31–40].

There is no clear evidence that black holes cannot exist in higher dimensions, and in dimensions higher than four, there are more degrees of freedom, so the uniqueness theorems do not hold. And the braneworld is an interesting high-dimensional cosmological model [41–43], which motivated by string theory (M-theory). The braneworld model has been proposed in which the standard fields are confined to a four-dimensional (4D) world viewed as a hypersurface (the brane) embedded in a higher-dimensional space-time (the bulk) through which only gravity can propagate [44, 45]. The apparent shape of rotating braneworld black holes were investigatedin [46, 47], and we have found a topologically charged rotating braneworld black hole in [48]. This black hole has two typs of charge, one arising from the bulk Weyl tensor and one from the gauge field trapped on the brane, which will cause interesting results.

This paper is organzied as follows. In section II, we briefly introduced the solution of the topologically charged rotating black hole and discussed the horizon. The geodesic equations and orbital equations of photons are given in section III. Further, we drew the photon region of the charged topological black hole and the black hole shadow in the section IV and section V respectively. In addition, we also

Preprints (www.preprints.org) | NOT PEER-REVIEWED | Posted: 30 September 2020

discussed the deformation of the black hole shadow and studied the energy emissivity. Finally, we summarize the work of the article in the section VI.

## II. TOPOLOGICALLY CHARGED ROTATING BRANEWORLD BLACK HOLE

The metric of a topologically charged rotating black hole in the Boyer-Lindquist coordinates reads

$$\begin{aligned} \mathrm{d}s^2 = \frac{\Delta - a^2\sin^2\theta}{\Sigma}\mathrm{d}t^2 - \frac{\Sigma}{\Delta}\mathrm{d}r^2 - \Sigma\mathrm{d}\theta^2 + 2a\sin^2\theta\left(1 - \frac{\Delta - a^2\sin^2\theta}{\Sigma}\right)\mathrm{d}t\mathrm{d}\varphi - \\ \sin^2\theta\left[\Sigma + a^2\sin^2\theta\left(2 - \frac{\Delta - a^2\sin^2\theta}{\Sigma}\right)\right]\mathrm{d}\varphi^2, \end{aligned} \tag{1}$$

with $\Delta$ and $\Sigma$ given by

$$\Delta = r^2 - 2Mr + a^2 + Q\left(r\right), \tag{2}$$

$$\Sigma = r^2 + a^2\cos^2\theta, \tag{3}$$

and

$$Q\left(r\right) = \beta + q^2 + \frac{\kappa_5^4 q^4}{240r^4}, \tag{4}$$

here $a$ is spin paramter, $\beta$ can be considered as a five-dimensional mass parameter, $q$ is the electric charge, and $\kappa_5^4$ is the five-dimensional gravity coupling constant. For the sake of calculation, we have chosen $\kappa_5^4 = 1$. The solution reduce to Schwarzschild solution when $a = 0$, $\beta = 0$ and $\kappa_5^4 = 0$.

As we can see,the metric is singular when $\Delta = 0$.

$$\Delta = r^2 - 2Mr + a^2 + \beta + q^2 + \frac{\kappa_5^4 q^4}{240r^4} = 0. \tag{5}$$

It can be seen from the above equation, the radii of horizons depend on the rotation paramter $a$ and the five-dimensional mass parameter $\beta$. Obviously, this

Preprints (www.preprints.org) | NOT PEER-REVIEWED | Posted: 30 September 2020

equation is unable to solved. However, the numerical analysis of Eq. (5) suggests the possibility of two roots of a set of values of parameters, which correspond the inner horizon $r_-$(smaller root) and the outer horizon $r_+$ (lager root), respectively. The variation of $\Delta$ with respect to $r$ for the different values.

The variation of $\Delta$ with respect to $r$ for different values of parameters $a$,with fixed $\beta$ and $q$ is depicted in Fig. 1. As can be seen from Fig. 1, for fixed parameters $\beta$ and $q$, the radii of outer horizon decrease with the increasing a while the radii of inner horizon increase when $a < a_E$. By calculating $\Delta = 0$ and $\frac{\mathrm{d}\Delta}{\mathrm{d}r} = 0$, we can obtain the critical rotation parameter $a_E$ and the corresponding critical radius $r_E$. Eq. (5) will have no root if $a > a_E$, inner horizon and outer horizo will disappear, in other words, the black hole will not exists any more.

We can analyze the other two parameters, $\beta$ and $q$, in the same way. And we can see the variation of $\Delta$ with respect to $r$ for different values of parameters $\beta$ (or $q$) with fixed $a$ in Fig. 2. Similar to changing parameter $a$, as $\beta$ (or $q$) increases, the distance between two horizons gradually decreases, when $\beta = \beta_E$ (or $q = q_E$), two horizons overlap and horizon will disappear if $\beta > \beta_E$ (or $q > q_E$).

## III. PHOTON ORBITS

In this section, we will give a brief introduction to the photon orbits in the topologically charged rotating black hole. In the black hole background, the geodesic equation can be governed by the Hamilton Jacobi equation,

$$\frac{\partial S}{\partial \lambda} = -\frac{1}{2} g^{\mu\nu} \frac{\partial S}{\partial x^\mu} \frac{\partial S}{\partial x^\nu}, \tag{6}$$

where $\lambda$ is the affine parameter, $x^\mu$ is expressed as the 4-vector, and the action $S$ which can be decomposed as a sum:

$$S = \frac{1}{2} m^2 \lambda - Et + L_\phi \phi + S_r(r) + S_\theta(\theta), \tag{7}$$

Preprints (www.preprints.org) | NOT PEER-REVIEWED | Posted: 30 September 2020

where $E$ and $L_\phi$ are, respectively, the energy and the angular momentum in the direction of the axis of symmetry. Substituting (7) into (6), one can obtain the equations of motion

$$\Sigma\frac{\mathrm{d}t}{\mathrm{d}\lambda}=\frac{-E\Sigma^2+aL_\phi\left(-\Delta+\Sigma\right)+a^2\left(aL_\phi+E\left(\Delta-2\Sigma\right)\right)\sin^2\theta-a^4E\sin^4\theta}{\Delta}, \tag{8}$$

$$\Sigma\frac{\mathrm{d}\phi}{\mathrm{d}\lambda}=-\frac{L_\phi}{\sin^2\theta}+\frac{a\left(aL_\phi+E\Delta-E\Sigma-a^2E\sin^2\theta\right)}{\Delta}, \tag{9}$$

$$\Sigma\frac{\mathrm{d}r}{\mathrm{d}\lambda}=\sqrt{\mathcal{R}}, \tag{10}$$

$$\Sigma\frac{\mathrm{d}\theta}{\mathrm{d}\lambda}=\sqrt{\Theta}, \tag{11}$$

where $\mathcal{R}$ and $\Theta$ are given by

$$\mathcal{R}=-\mathcal{K}\Delta-\Delta\left(L_\phi-aE\right)^2+\left(aL_\phi-\left(a^2+r^2\right)E\right)^2, \tag{12}$$

$$\Theta=\mathcal{K}+L_\phi^2+a^2E^2\cos^2\theta-\frac{L_\phi^2}{\sin^2\theta}, \tag{13}$$

with $\mathcal{K}$ denoting the Carter constant. Since the spacetime is asymptotically flat, the photon path is a straight line at infinity. However, when there a black hole is placed between the observer and the light source, the light will reach the observer after deflecting due to the strong gravitational field of the black hole. And now, we are going to discuss the radial motion of photon.

The motion of photon is determined by two impact parameters $\xi=L_\phi/E$ and $\eta=\mathcal{K}/E$. From Eq. (10), we can obtain the circular photon orbits, which are very useful on determining the shape of black hole shadow. The conditions for these orbits are

$$\mathcal{R}=0,\frac{\mathrm{d}\mathcal{R}}{\mathrm{d}r}=0, \tag{14}$$

from above questions, we get

$$\xi=a+\frac{r^2}{a}-\frac{4r\Delta}{a\Delta'}, \tag{15}$$

Preprints (www.preprints.org) | NOT PEER-REVIEWED | Posted: 30 September 2020

## IV. PHOTON REGIONS

Now, we are interested in spherical null geodesics, i.e., null geodesics that stay on a sphere $r$ =constant. Inserting these expression (15) and (16) into (13), which gives us an inequality that calculation the photon region $\mathscr{K}$:

$$\mathscr{K} : 16a^2r^2\Delta\sin^2(\theta) \geq (4r\Delta - \Sigma\Delta')\,. \tag{17}$$

A spherical null geodesic at $r = r_p$ is unstable with respect to radial perturbations if $R''(r_p) > 0$, and stable if $R''(r_p) < 0$. From Eq. (12), we can calculate the second derivative $R''$

$$\frac{\mathcal{R}''}{8E^2}\Delta'^2 = 2r\Delta\Delta' + r^2\Delta'^2 - 2r^2\Delta\Delta''. \tag{18}$$

When drawing according to the above formula, we used the coordinate transformation in [49], so that the entire space-time can be displayed. And we show the photon regions of the topologically charged rotating black hole in Fig. 4, Fig. 5 and Fig. 6, the meaning of the different areas in these images is explained in Fig. 3.

In Fig. 4, we show the effect on the photon regions when the parameter $a$ takes different values. Due to coordinate transformation, the photon regions are divided into two parts, interior photon region ($r < r_-$) and exterior photon region ($r > r_+$), and they are symmetrical about the coordinate axis. It can be seen that when the value of $a$ is very small, the photon regions degenerate into photon spheres. If the parameters $\beta$ and $q$ are zero at this time, the image describes the Schwarzschild case, and the radius of the photon spheres is $r = 3M$, that is, the coordinates marked on the figure are $(\pm 4, 0)$.

When $a \neq 0$, the exterior photon region gradually changes from a spherical shape to a crescent shape, and grows with increasing $a$. The interior photon region consists of two connected components that are separated by the ring singularity.

Preprints (www.preprints.org) | NOT PEER-REVIEWED | Posted: 30 September 2020

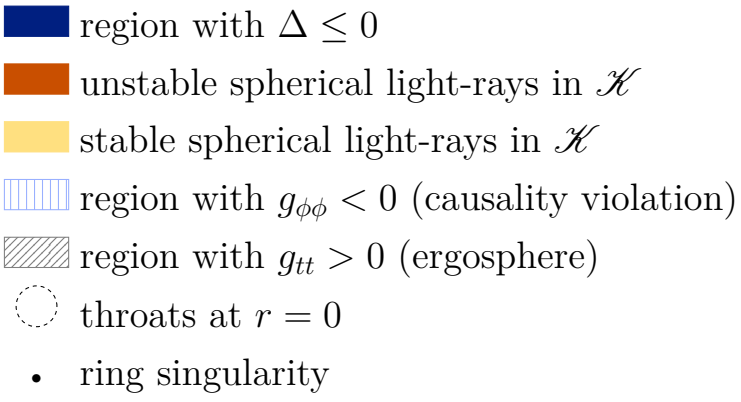


Figure 3: Legend for Figs.4, 5 and 6

Unlike the case where there is only unstable spherical light-rays in exterior photon region, there are two regions of stable and unstable in interior photon region at the same time. With $a$ increased, the distance between the internal and external horizon gradually decreases. When $\beta = q = 0$, the shape of the photon region is similar to Kerr case. If $\beta$ or $q$ is not zero, the shape of the region with $g_{\phi\phi} < 0$ will be significantly deformed. In Figs. 5 and 6, we show the influence of parameters $\beta$ and $q$ on the shape of various regions, respectively. As shown in Fig. 5, when $\beta \neq 0$, the shape of the region with $g_{\phi\phi} < 0$ are not deformed. But in Fig. 6, as $q$ increases, the deformation becomes more obvious.

## V. SHADOW OF BLACK HOLE

### A. The shadow shape

As mentioned earlier, if a black hole located between a light source and an observer, due to the strong gravity of the black hole, the light path will no longer be a straight line. There will be three situations for this impact, when a photon is

Preprints (www.preprints.org) | NOT PEER-REVIEWED | Posted: 30 September 2020

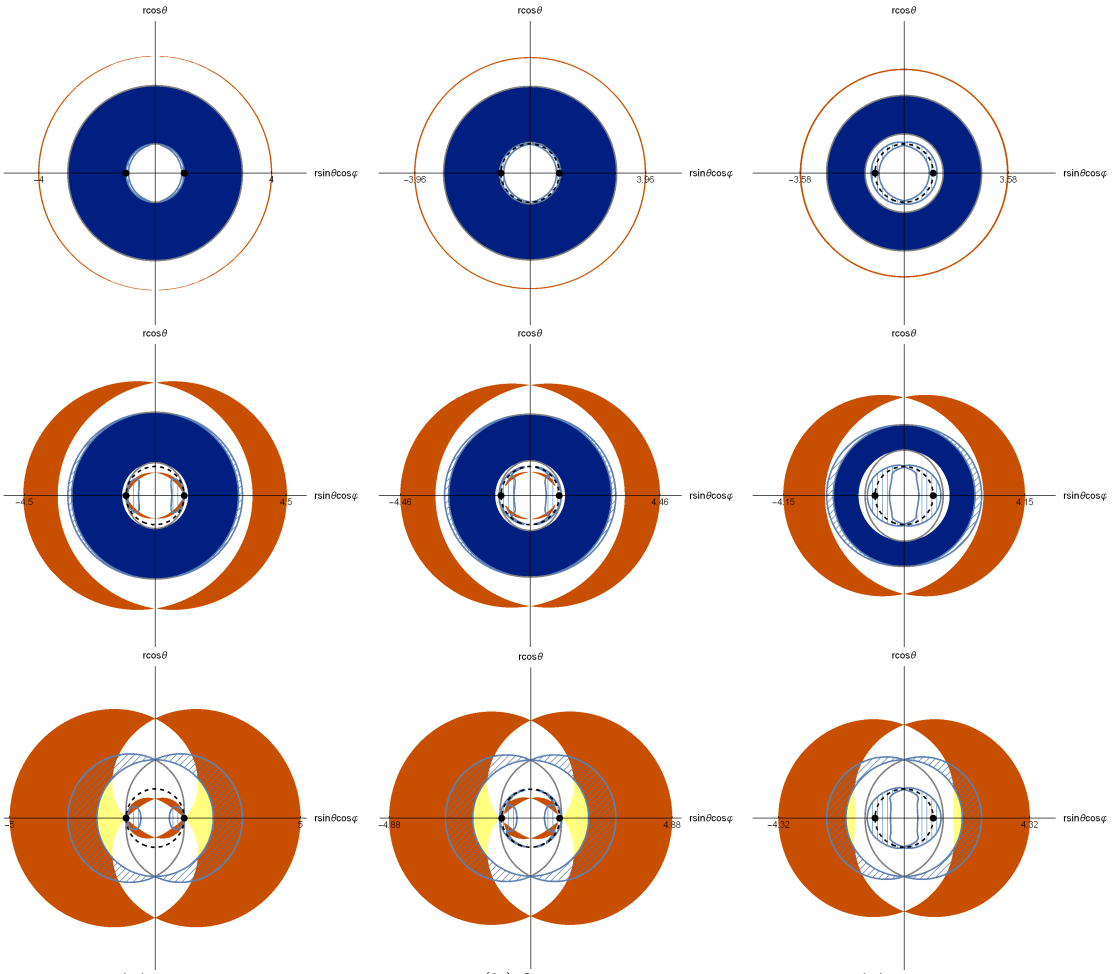


(a)$\beta$=q=0 (b)$\beta$=q=0.1 (c)$\beta$=q=0.4

Figure 4: The shapes of the photon regions for different values of the parameters. The first line, $a = 0.02$. The second line, $a = 0.5$. The thrid line, $a = a_{Max}$.

emitted from a light source at infinity and bypasses the black hole. In first case, with a large enough orbital angular momentum, the photon will turn around and reach the observer at infinity. For the second case, the orbital angular momentum of the photon is too small to resist the gravity and the photon will fall into the black hole, thus the ovserver cannot see the light source. If there are countless evenly

Preprints (www.preprints.org) | NOT PEER-REVIEWED | Posted: 30 September 2020

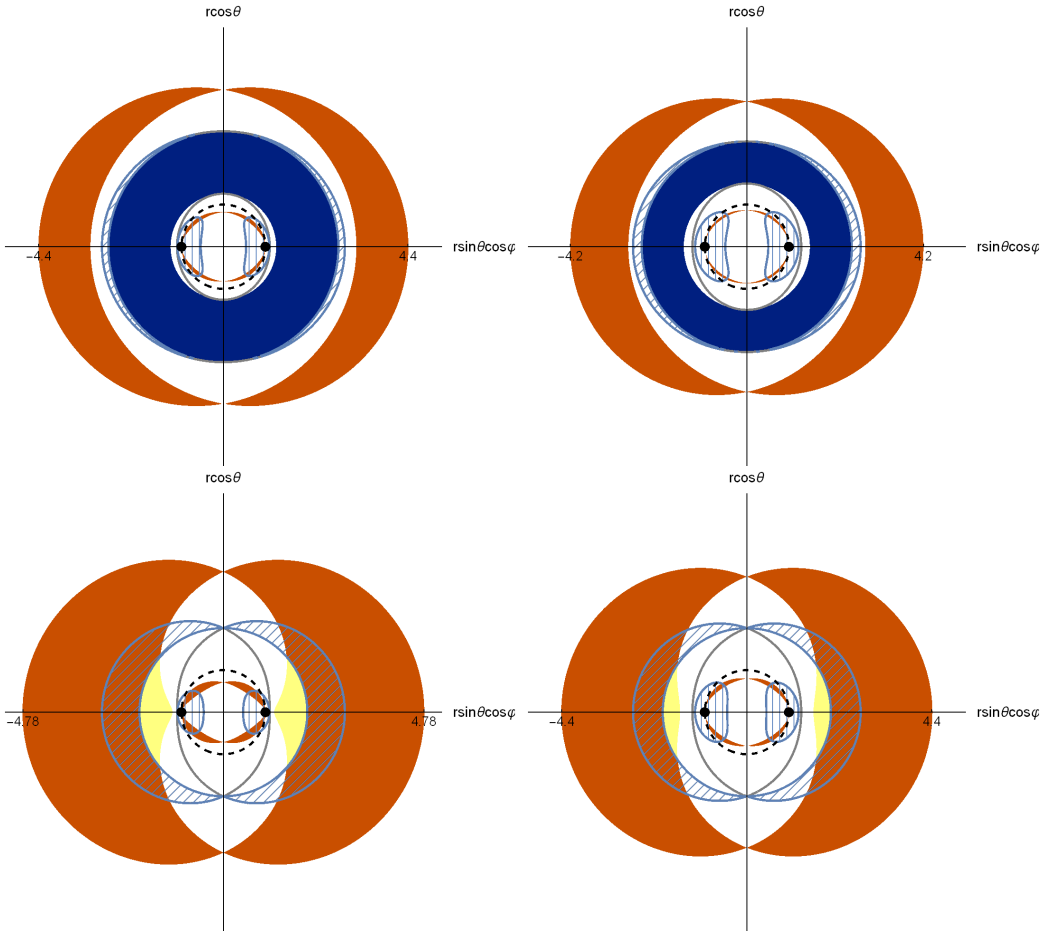


(a)$\beta$=0.2,q=0 (b)$\beta$=0.5,q=0

Figure 5: The shapes of the photon regions for different values of $\beta$. The first line, $a = 0.5$. The second line, $a = a_{Max}$.

distributed light sources at infinity, because of the second case, the observer will see a dark zone, which is the shadow of the black hole.The third case, the orbital angular momentum is in a critical state, which makes the photon always move around the black hole instead of escaping or falling into the black hole. This critical state will help us define the boundary of the shadow.

Preprints (www.preprints.org) | NOT PEER-REVIEWED | Posted: 30 September 2020

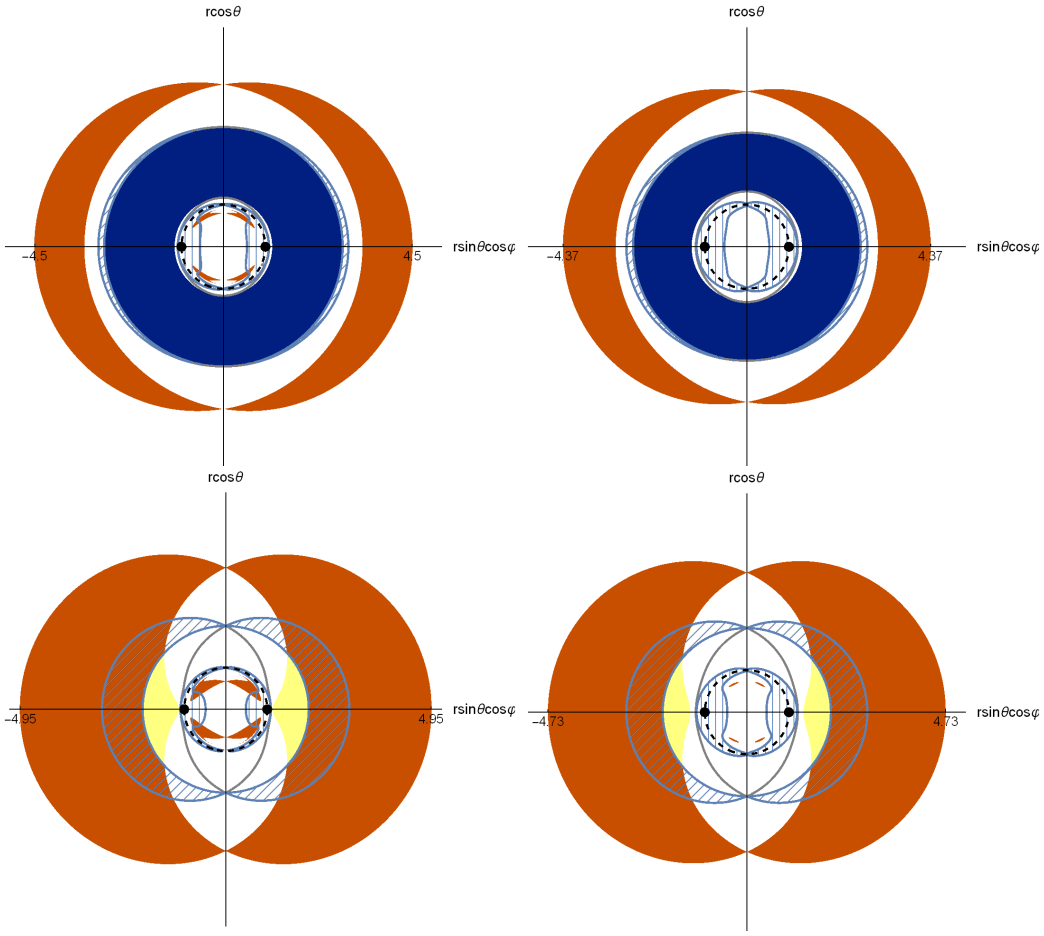


(a)$\beta$=0,q=0.2 (b)$\beta$=0,q=0.5

Figure 6: The shapes of the photon regions for different values of $q$. The first line, $a = 0.5$. The second line, $a = a_{Max}$.

For depicting the shadows, we use a stereographic projection from the celestial sphere onto to a plane with the Cartesian coordinates [50]:

$$\begin{aligned} x &= -\xi \csc\theta, \\ y &= \pm\sqrt{\eta + a^2\cos^2\theta - \xi^2\cot^2\theta}, \end{aligned} \tag{19}$$

the angle between the line of sight of observer and the black hole's rotation axis is $\theta$.

Preprints (www.preprints.org) | NOT PEER-REVIEWED | Posted: 30 September 2020

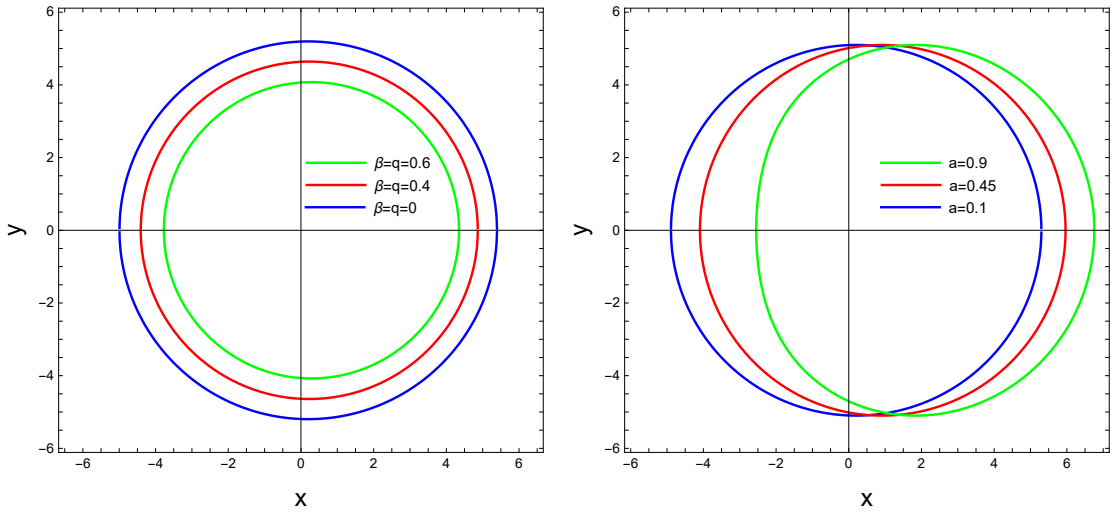


(a) (b)

Figure 7: Shadows cast by black holes. (a) The non-rotating case ($a = 0$). (b)$a \neq 0$, $\beta = q = 0$.

defined as

$$R_s = \frac{(x_t - x_r)^2 + y_t^2}{2\,(x_r - x_t)}. \tag{20}$$

We numerically calculate these observables, and the radius $R_s$ is clearly shown in Fig. 10. In Fig. 10(a), we can find that for fixed $q$, $R_s$ increases with the spin parameter $a$ and decreases as the five-dimensional mass parameter $\beta$. Fig. 10(b) further shows this trend. This is because parameter $\beta$ makes the shadow shape smaller, and parameter $a$ increases the deformation of the shadow shape as shown above. At the same time, we show that for fixed a, $R_s$ will also decreases as the electric charge parameter $q$, just like $\beta$. Interestingly, the result shows that the shadow of a topologically charged rotating black hole is smaller.

The distortion parameter $\delta_s$ are clearly shown in Fig. 11. As shown in Fig. 11(a) and Fig. 11(b), when the parameter $a$ is fixed to a larger value, the shape of

Preprints (www.preprints.org) | NOT PEER-REVIEWED | Posted: 30 September 2020

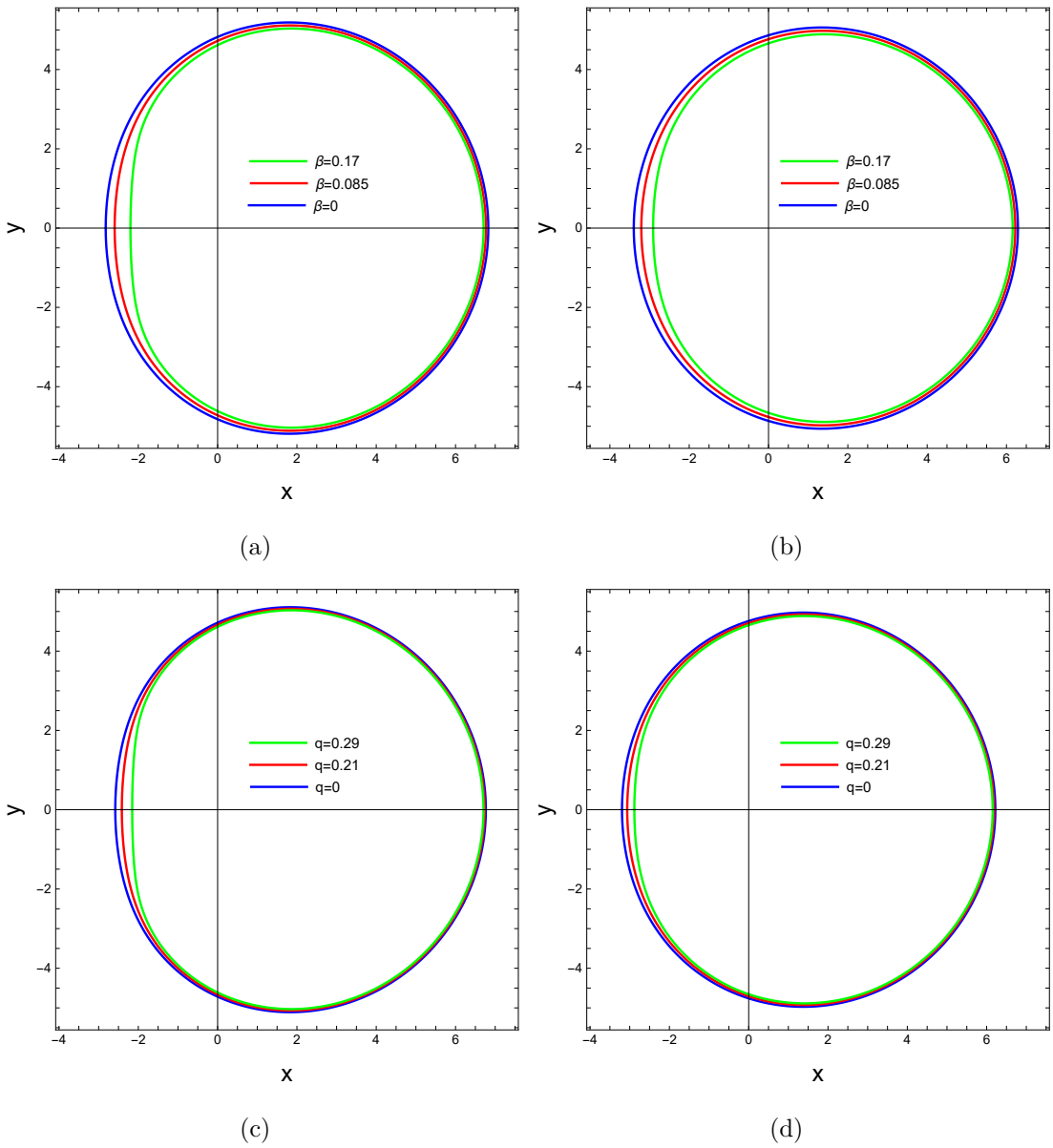


Figure 8: The shapes of the black hole shadow for different values of the parameters. (a) $a = 0.9, q = 0.1, \theta = \pi/2$. (b) $a = 0.9, q = 0.1, \theta = \pi/4$. (c) $a = 0.9, \beta = 0.1, \theta = \pi/2$. (d) $a = 0.9, \beta = 0.1, \theta = \pi/4$.

Preprints (www.preprints.org) | NOT PEER-REVIEWED | Posted: 30 September 2020

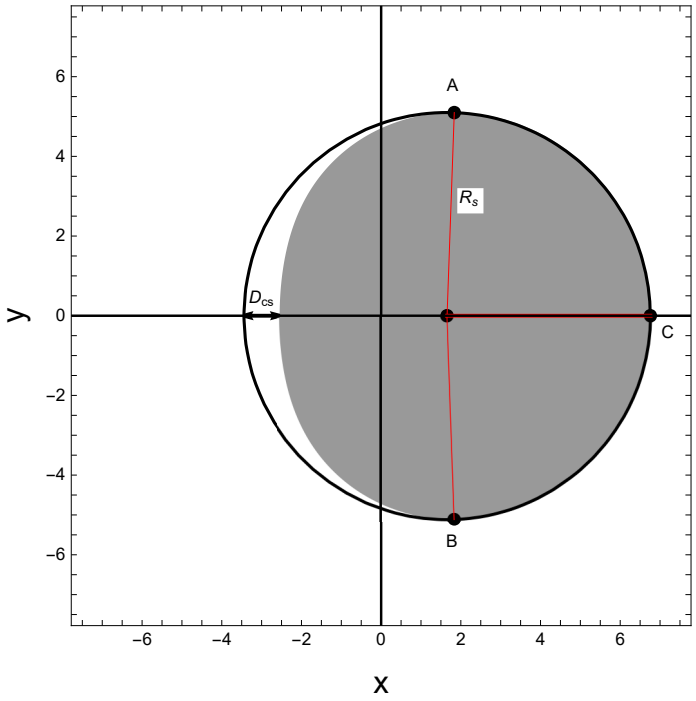


Figure 9: The observable parameter, the radius $R_s$(red line), and the distortion parameter $\delta_s = D_{cs}/R_s$ are described as the apparent shape of the black hole.

the shadow is obviously deformed, regardless of the parameters $\beta$ or $q$, their increase will exacerbate the deformation of the shadow shape, and the effect of $q$ is more obvious. And in Fig. 11(c), for fixed the parameters $\beta$ and $q$, $\delta_s$ increases with the spin parameter $a$.

From [51], the authors proposed that the area of the black hole shadow is approximately equal to the high-energy absorption cross-section for an observer at the equatorial plane at infinity. According to this assumption, the energy emission rate of the black hole in high energy case is

$$\frac{\mathrm{d}^2 E(\omega)}{\mathrm{d}\omega \mathrm{d}t} = \frac{2\pi^3 R_s^2}{e^{\omega/T_H} - 1}\omega^3, \tag{21}$$

where $R_s$ is given in Eq. (20), and $T_H$ is the Hawking temperature, which in [48]

Preprints (www.preprints.org) | NOT PEER-REVIEWED | Posted: 30 September 2020

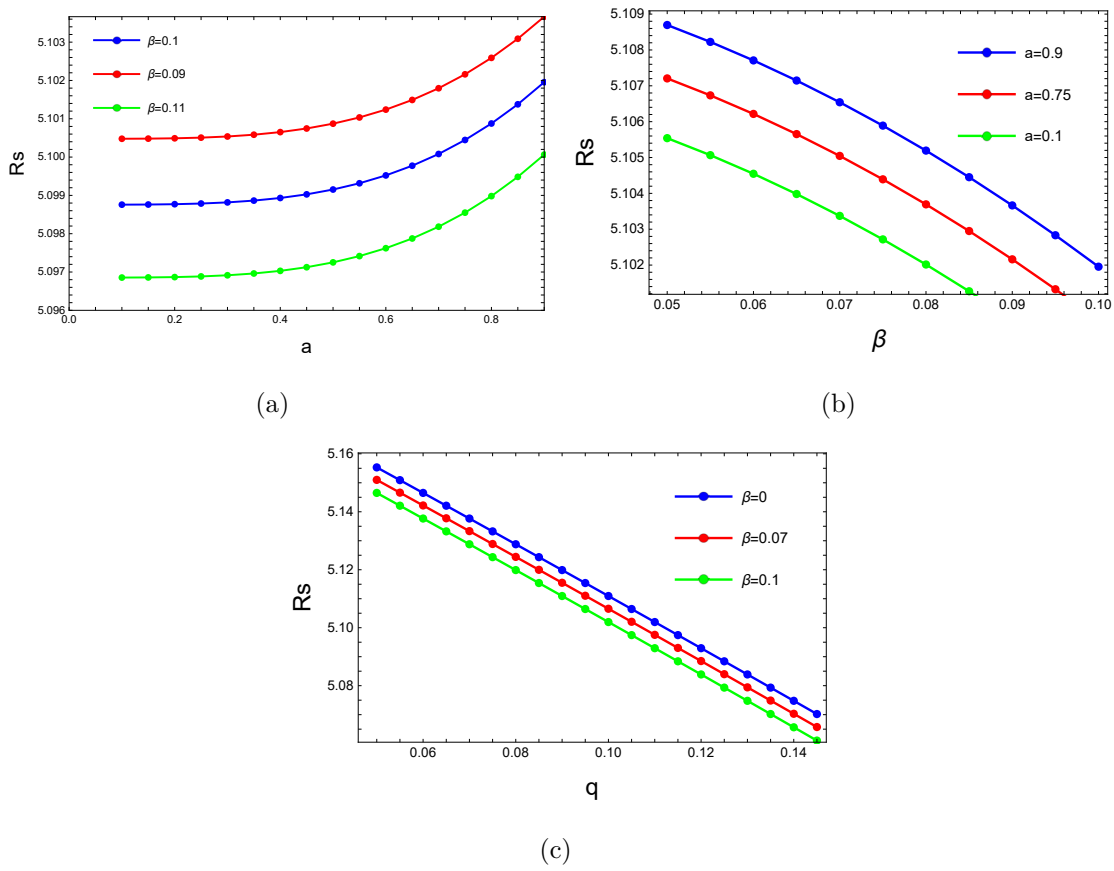


Figure 10: (a) The radius $R_s$ of the black hole shadow against $a$ for different values of parameter $\beta$, $q = 0.1$. (b) $R_s$ against $\beta$ for different values of parameter $a$, $q = 0.1$. (c) $R_s$ against $q$ tfor different values of parameter $\beta$, $a = 0.9$.

given by

$$T = \frac{r_+}{4\pi\left(r_+^2 + a^2\right)}\left(1 - \frac{a^2}{r_+^2} - \frac{\beta + q^2}{r_+^2} - \frac{1}{48}\frac{\kappa_5^4 q^4}{r_+^6}\right), \tag{22}$$

then, we discribe the energy emission rate against the frequency $\omega$ for different parameters respectively, a, $\beta$ and q, in Fig. 12. For each parameter, the curve has a peak. And the peak will decrease as the corresponding parameter increases, when the other two parameters are fixed.

Preprints (www.preprints.org) | NOT PEER-REVIEWED | Posted: 30 September 2020

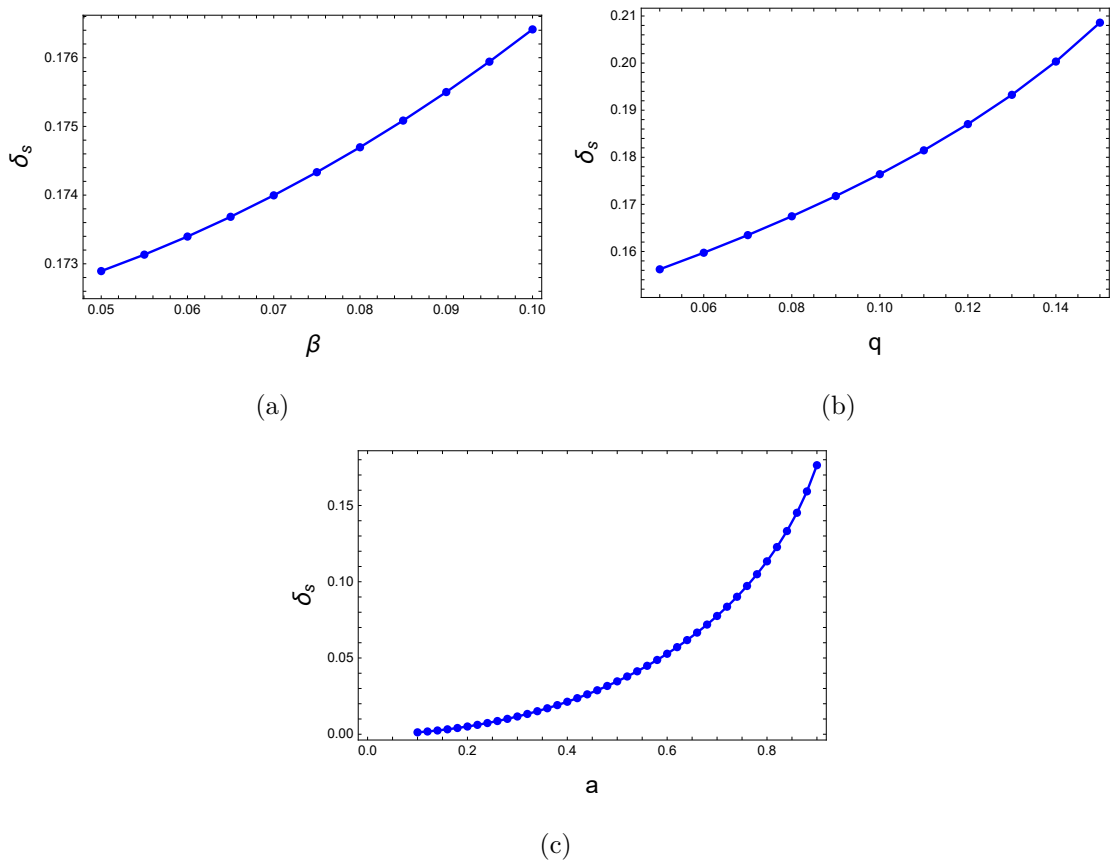


Figure 11: The distortion $\delta_s$ of the black hole shadow for different values of the parameters. (a)$a = 0.9$, $q = 0.1$. (b)$a = 0.9$, $q = 0.1$. (c)$\beta = q = 0.1$.

## VI. CONCLUSIONS AND DISCUSSIONS

In this paper, we have obtained the solution of a topologically charged rotating black hole. Through this solution, we have discussed horizon of the black hole. It can be seen that as the parameter increases, the distance between two hroizons will gradually decrease.

Then we studied the photon region, which is a standard circle in the Schwarzschild case, and splits in the rotating case. This is also the reason for the deformation of

Preprints (www.preprints.org) | NOT PEER-REVIEWED | Posted: 30 September 2020

is equal to the high-energy absorption cross section, based on this assumption, we studied the energy emission rate. From the figure, one can find that with the incerase of parameters $a$, $\beta$ and $q$, the peak decreases and moves to the low frequency.

With the improvement of the observation level, it is believed that more observational data of the massive black hole in the center of the galaxy will be obtained in the future. These data will help scientists verify the existing gravitational theories, so our work may provide a tool for observation of braneworld model or charged black holes.

## CONFLICTS OF INTEREST

The authors declare that there are no conflicts of interest regarding the publication of this paper.

## ACKNOWLEDGMENTS

We would like to thank the National Natural Science Foundation of China (Grant No.11571342) for supporting us on this work. This work makes use of the Black Hole Perturbation Toolkit.

## REFERENCES

[1] Event Horizon Telescope Collaboration et al. First m87 event horizon telescope results. i. the shadow of the supermassive black hole. *arXiv preprint arXiv:1906.11238*, 2019.

Preprints (www.preprints.org) | NOT PEER-REVIEWED | Posted: 30 September 2020

[2] Kazunori Akiyama, Antxon Alberdi, Walter Alef, Keiichi Asada, Rebecca Azulay, Anne-Kathrin Baczko, David Ball, Mislav Baloković, John Barrett, Dan Bintley, et al. First m87 event horizon telescope results. ii. array and instrumentation. *The Astrophysical Journal Letters*, 875(1):L2, 2019.

[3] Kazunori Akiyama, Antxon Alberdi, Walter Alef, Keiichi Asada, Rebecca Azulay, Anne-Kathrin Baczko, David Ball, Mislav Baloković, John Barrett, Dan Bintley, et al. First m87 event horizon telescope results. iii. data processing and calibration. *The Astrophysical Journal Letters*, 875(1):L3, 2019.

[4] Kazunori Akiyama, Antxon Alberdi, Walter Alef, Keiichi Asada, Rebecca Azulay, Anne-Kathrin Baczko, David Ball, Mislav Baloković, John Barrett, Dan Bintley, et al. First m87 event horizon telescope results. iv. imaging the central supermassive black hole. *The Astrophysical Journal Letters*, 875(1):L4, 2019.

[5] Kazunori Akiyama, Antxon Alberdi, Walter Alef, Keiichi Asada, Rebecca Azulay, Anne-Kathrin Baczko, David Ball, Mislav Baloković, John Barrett, Dan Bintley, et al. First m87 event horizon telescope results. v. physical origin of the asymmetric ring. *The Astrophysical Journal Letters*, 875(1):L5, 2019.

[6] Kazunori Akiyama, Antxon Alberdi, Walter Alef, Keiichi Asada, Rebecca Azulay, Anne-Kathrin Baczko, David Ball, Mislav Baloković, John Barrett, Dan Bintley, et al. First m87 event horizon telescope results. vi. the shadow and mass of the central black hole. *The Astrophysical Journal Letters*, 875(1):L6, 2019.

[7] Edward Teo. Spherical photon orbits around a kerr black hole. *General Relativity and Gravitation*, 35(11):1909–1926, 2003.

[8] Volker Perlick. Gravitational lensing from a spacetime perspective. *Living reviews in relativity*, 7(1):9, 2004.

[9] Arne Grenzebach, Volker Perlick, and Claus Lämmerzahl. Photon regions and shadows of kerr-newman-nut black holes with a cosmological constant. *Physical Review D*,

Preprints (www.preprints.org) | NOT PEER-REVIEWED | Posted: 30 September 2020

89(12):124004, 2014.

[10] Virginia Trimble. The shadow of black holes: An analytic description, 2017.

[11] JM Bardeen. Black holes, proceedings of the les houches summer school, session 215239. 1973.

[12] Charles Galton Darwin. The gravity field of a particle. *Proceedings of the Royal Society of London. Series A. Mathematical and Physical Sciences*, 249(1257):180–194, 1959.

[13] Hans C Ohanian. The black hole as a gravitational ‘‘lens’’. *American Journal of Physics*, 55(5):428–432, 1987.

[14] Robert J Nemiroff. Visual distortions near a neutron star and black hole. *American Journal of Physics*, 61(7):619–632, 1993.

[15] Valerio Bozza, S Capozziello, G Iovane, and G Scarpetta. Strong field limit of black hole gravitational lensing. *General Relativity and Gravitation*, 33(9):1535–1548, 2001.

[16] Valerio Bozza. Gravitational lensing by black holes. *General Relativity and Gravitation*, 42(9):2269–2300, 2010.

[17] KS Virbhadra. Relativistic images of schwarzschild black hole lensing. *Physical Review D*, 79(8):083004, 2009.

[18] VS Morozova, BJ Ahmedov, and AA Tursunov. Gravitational lensing by a rotating massive object in a plasma. *Astrophysics and Space Science*, 346(2):513–520, 2013.

[19] Oleg Yu Tsupko and Gennady S Bisnovatyi-Kogan. Gravitational lensing in plasma: Relativistic images at homogeneous plasma. *Physical Review D*, 87(12):124009, 2013.

[20] Heino Falcke, Fulvio Melia, and Eric Agol. Viewing the shadow of the black hole at the galactic center. *The Astrophysical Journal Letters*, 528(1):L13, 1999.

[21] Subrahmanyan Chandrasekhar. *The mathematical theory of black holes*, volume 69. Oxford University Press, 1998.

Preprints (www.preprints.org) | NOT PEER-REVIEWED | Posted: 30 September 2020

[22] Petya G Nedkova, Vassil K Tinchev, and Stoytcho S Yazadjiev. Shadow of a rotating traversable wormhole. *Physical Review D*, 88(12):124019, 2013.

[23] Cosimo Bambi and Katherine Freese. Apparent shape of super-spinning black holes. *Physical Review D*, 79(4):043002, 2009.

[24] Alexander F Zakharov, AA Nucita, F DePaolis, and G Ingrosso. Measuring the black hole parameters in the galactic center with radioastron. *New Astronomy*, 10(6):479–489, 2005.

[25] AF Zakharov, F De Paolis, G Ingrosso, and AA Nucita. Direct measurements of black hole charge with future astrometrical missions. *Astronomy & Astrophysics*, 442(3):795–799, 2005.

[26] F De Paolis, G Ingrosso, AA Nucita, A Qadir, and AF Zakharov. Estimating the parameters of the sgr a* black hole. *General Relativity and Gravitation*, 43(4):977–988, 2011.

[27] A De Vries. The apparent shape of a rotating charged black hole, closed photon orbits and the bifurcation set a4. *Classical and Quantum Gravity*, 17(1):123, 2000.

[28] Kenta Hioki and Kei-ichi Maeda. Measurement of the kerr spin parameter by observation of a compact object's shadow. *Physical Review D*, 80(2):024042, 2009.

[29] Akifumi Yumoto, Daisuke Nitta, Takeshi Chiba, and Naoshi Sugiyama. Shadows of multi-black holes: analytic exploration. *Physical Review D*, 86(10):103001, 2012.

[30] Ahmadjon Abdujabbarov, Farruh Atamurotov, Yusuf Kucukakca, Bobomurat Ahmedov, and Ugur Camci. Shadow of kerr-taub-nut black hole. *Astrophysics and Space Science*, 344(2):429–435, 2013.

[31] Shao-Wen Wei and Yu-Xiao Liu. Testing the nature of gauss-bonnet gravity by four-dimensional rotating black hole shadow. *arXiv preprint arXiv:2003.07769*, 2020.

[32] He-Xu Zhang, Cong Li, Peng-Zhang He, Qi-Qi Fan, and Jian-Bo Deng. Optical properties of a brane-world black hole as photons couple to the weyl tensor. *European*

Preprints (www.preprints.org) | NOT PEER-REVIEWED | Posted: 30 September 2020

*Physical Journal C*, 80(5):1–11, 2020.

[33] Yuan Chen, He-Xu Zhang, Tian-Chi Ma, and Jian-Bo Deng. Optical properties of a nonlinear magnetic charged rotating black hole surrounded by quintessence with a cosmological constant. *arXiv preprint arXiv:2009.03778*, 2020.

[34] Kenta Hioki and Umpei Miyamoto. Hidden symmetries, null geodesics, and photon capture in the sen black hole. *Physical Review D*, 78(4):044007, 2008.

[35] Leonardo Amarilla, Ernesto F Eiroa, and Gaston Giribet. Null geodesics and shadow of a rotating black hole in extended chern-simons modified gravity. *Physical Review D*, 81(12):124045, 2010.

[36] Farruh Atamurotov, Ahmadjon Abdujabbarov, and Bobomurat Ahmedov. Shadow of rotating non-kerr black hole. *Physical Review D*, 88(6):064004, 2013.

[37] Uma Papnoi, Farruh Atamurotov, Sushant G Ghosh, and Bobomurat Ahmedov. Shadow of five-dimensional rotating myers-perry black hole. *Physical Review D*, 90(2):024073, 2014.

[38] Rajibul Shaikh. Shadows of rotating wormholes. *Physical Review D*, 98(2):024044, 2018.

[39] Shohreh Abdolrahimi, Robert B Mann, and Christos Tzounis. Distorted local shadows. *Physical Review D*, 91(8):084052, 2015.

[40] Farruh Atamurotov, Bobomurat Ahmedov, and Ahmadjon Abdujabbarov. Optical properties of black holes in the presence of a plasma: The shadow. *Physical Review D*, 92(8):084005, 2015.

[41] David Langlois. Brane cosmology. *Progress of Theoretical Physics Supplement*, 148:181–212, 2002.

[42] Philippe Brax and Carsten van de Bruck. Cosmology and brane worlds: a review. *Classical and Quantum Gravity*, 20(9):R201, 2003.

Preprints (www.preprints.org) | NOT PEER-REVIEWED | Posted: 30 September 2020

[43] Roy Maartens and Kazuya Koyama. Brane-world gravity. *Living Reviews in Relativity*, 13(1):5, 2010.

[44] Valerii A Rubakov. Large and infinite extra dimensions. *Physics-Uspekhi*, 44(9):871, 2001.

[45] Csaba Csaki. Tasi lectures on extra dimensions and branes. *arXiv preprint hep-ph/0404096*, 2004.

[46] Leonardo Amarilla and Ernesto F Eiroa. Shadow of a rotating braneworld black hole. *Physical Review D*, 85(6):064019, 2012.

[47] Jan Schee and Zdeněk Stuchlík. Optical phenomena in the field of braneworld kerr black holes. *International Journal of Modern Physics D*, 18(06):983–1024, 2009.

[48] A Larranaga, C Grisales, and M Londono. A topologically charged rotating black hole in the brane, adv. *High Energy Phys*, 727294, 2013.

[49] Barrett O'Neill. The geometry of kerr black holes, ak peters ltd. *Wellesley, MA*, 1995.

[50] Hui-Min Wang, Yu-Meng Xu, and Shao-Wen Wei. Shadows of kerr-like black holes in a modified gravity theory. *Journal of Cosmology and Astroparticle Physics*, 2019(03):046, 2019.

[51] Shao-Wen Wei and Yu-Xiao Liu. Observing the shadow of einstein-maxwell-dilaton-axion black hole. *Journal of Cosmology and Astroparticle Physics*, 2013(11):063, 2013.